Published by Institute of Physics Publishing for SISSA/ISAS
Received: *August 28, 2002*
Accepted: *August 30, 2002*

The double radiative decays $B \to \gamma\gamma$ in the heavy quark limit

Stefan W. Bosch

Max-Planck-Institut für Physik, Werner-Heisenberg-Institut
Föhringer Ring 6, D-80805 Munich, Germany
E-mail: stefan.bosch@cern.ch

Gerhard Buchalla

Ludwig-Maximilians-Universität München, Sektion Physik
Theresienstraße 37, D-80333 Munich, Germany
E-mail: buchalla@theorie.physik.uni-muenchen.de

Abstract: We analyze the double radiative B-meson decays $B_s \to \gamma\gamma$ and $B_d \to \gamma\gamma$ in QCD factorization based on the heavy-quark limit $m_b \gg \Lambda_{QCD}$. We systematically discuss the various contributions to these exclusive processes. The dominant effect arises from the magnetic-moment type transition $b \to s(d)\gamma$ where an additional photon is emitted from the light quark (one-particle reducible diagram). The contributions from one-particle irreducible diagrams are power suppressed. We argue that they are still calculable within QCD factorization. They are used to compute the CP-asymmetry in $B \to \gamma\gamma$ and to estimate so-called long-distance contributions in B and $D \to \gamma\gamma$. Numerical results are presented for branching ratios and CP asymmetries.

Keywords: B-Physics, Heavy Quarks Physics, Rare Decays.

JHEP08(2002)054

© SISSA/ISAS 2002

Contents

1. Introduction **1**

2. Basic formulas **2**

3. $B \to \gamma\gamma$ at leading power **5**

4. Contributions to $B \to \gamma\gamma$ with power suppression **6**

5. Long-distance contributions to $B \to \gamma\gamma$ and $D \to \gamma\gamma$ **10**

6. Phenomenology **12**

7. Conclusions **15**

1. Introduction

The rare decays of B mesons provide an excellent means to further explore the Standard Model (SM) and to detect New Physics. In particular the Cabibbo-favoured radiative $b \to s\gamma$ modes belong to the small number of rare decays that are experimentally accessible already at present [1]–[4] and give severe bounds on the parameter space of New Physics scenarios. On the theoretical side both the inclusive [5]–[7] and exclusive [8]–[10] $b \to s\gamma$ decays are now known at next-to-leading-logarithmic (NLL) accuracy.

For the double radiative decays $B \to \gamma\gamma$ experimentally so far only upper limits on the branching fractions exist:

$$\begin{aligned} B(B_s \to \gamma\gamma) &< 1.48 \cdot 10^{-4} \text{ at } 90\% \text{ C.L.} \quad [11] \\ B(B_d \to \gamma\gamma) &< 1.7 \cdot 10^{-6} \quad \text{at } 90\% \text{ C.L.} \quad [12]\,. \end{aligned} \tag{1.1}$$

The Standard Model expectations are roughly two orders below the current upper limits. These decays have a rather clean experimental signature. Furthermore they are of interest because they could provide useful tests of QCD dynamics in B decays. The $B \to \gamma\gamma$ modes realize the exceptional situation of nontrivial QCD dynamics related to the decaying B, in conjunction with a completely nonhadronic final state and simple two-body kinematics. In principle they also probe the CKM parameters V_{ts} and V_{td} and could allow us to study CP violating effects as the two-photon system can be in a CP-even or CP-odd state. While contributions of New Physics to $B_s \to \gamma\gamma$ are strongly constrained by the measurements of $b \to s\gamma$ transitions, a sizable enhancement of $B_d \to \gamma\gamma$ from effects beyond the Standard Model is still conceivable.

JHEP08(2002)054

The theoretical treatments of $B_s \to \gamma\gamma$ performed so far [13]–[22] all had to employ hadronic models to describe the B_s meson bound state dynamics. A clear separation of short- and long-distance dynamics and a distinction of model-dependent and model-independent features were therefore not possible. This concerns especially the dynamics of the light-quark constituent inside the B, but also contributions from intermediate J/ψ, η_c, ϕ or $D_s^{(*)}$ meson states, which have been discussed as sources of potentially important long-distance effects. Another process related to $B \to \gamma\gamma$ is the decay $B \to l^+l^-\gamma$. This decay has recently been studied in [23].

We present in this paper a systematic analysis of the exclusive double radiative decays $B_{s,d} \to \gamma\gamma$ in QCD, based on the heavy quark limit $m_b \gg \Lambda_{QCD}$. This limit allows us to give a factorization formula for the hadronic matrix elements of local operators in the weak hamiltonian [8, 9, 10, 24]. In this manner we can systematically separate perturbatively calculable hard scattering kernels from the nonperturbative B-meson light-cone distribution amplitude (LCDA). Power counting in Λ_{QCD}/m_b allows us to identify leading and subleading contributions to $B \to \gamma\gamma$. Only one diagram contributes at leading power, but the most important subleading contributions can also be calculated. The inclusion of these corrections is used to estimate CP asymmetries in $B \to \gamma\gamma$ and one-particle irreducible two-photon emission from light-quark loops in $D \to \gamma\gamma$. These corrections represent the quark-level analogue of so-called long-distance contributions in these decays.

The remainder of this paper is organized as follows. In section 2 we give the basic formulas necessary for the calculation of the observables of interest. Section 3 contains our discussion of leading-power and section 4 the one of subleading-power contributions. In section 5 we comment on long-distance contributions in $B \to \gamma\gamma$ and $D \to \gamma\gamma$ decays. Numerical results are presented and discussed in section 6. Section 7 contains our conclusions.

2. Basic formulas

The effective hamiltonian for $b \to s\gamma\gamma$ is identical to the one for $b \to s\gamma$ transitions. This is because the equations of motion (EOM) can be used to reduce the basis with operators containing two photon fields [25]. Up to corrections of order $1/M_W^2$ the effective hamiltonian thus reads

$$\mathcal{H}_{\text{eff}} = \frac{G_F}{\sqrt{2}} \sum_{p=u,c} \lambda_p^{(s)} \left[C_1 Q_1^p + C_2 Q_2^p + \sum_{i=3,\ldots,8} C_i Q_i \right] + \text{h.c.} \tag{2.1}$$

where

$$\lambda_p^{(s)} = V_{ps}^* V_{pb} \,. \tag{2.2}$$

The operators are given by

$$Q_1^p = (\bar{s}p)_{V-A}(\bar{p}b)_{V-A} \tag{2.3}$$

$$Q_2^p = (\bar{s}_i p_j)_{V-A}(\bar{p}_j b_i)_{V-A} \tag{2.4}$$

$$Q_3 = (\bar{s}b)_{V-A} \sum_q (\bar{q}q)_{V-A} \tag{2.5}$$

JHEP08(2002)054

$$Q_4 = (\bar{s}_i b_j)_{V-A} \sum_q (\bar{q}_j q_i)_{V-A} \tag{2.6}$$

$$Q_5 = (\bar{s} b)_{V-A} \sum_q (\bar{q} q)_{V+A} \tag{2.7}$$

$$Q_6 = (\bar{s}_i b_j)_{V-A} \sum_q (\bar{q}_j q_i)_{V+A} \tag{2.8}$$

$$Q_7 = \frac{e}{8\pi^2} m_b \, \bar{s}_i \sigma^{\mu\nu} (1+\gamma_5) b_i \, F_{\mu\nu} \tag{2.9}$$

$$Q_8 = \frac{g}{8\pi^2} m_b \, \bar{s}_i \sigma^{\mu\nu} (1+\gamma_5) T^a_{ij} b_j \, G^a_{\mu\nu} \, . \tag{2.10}$$

The most important operators are the magnetic penguin operator Q_7 and the four-quark operators $Q^p_{1,2}$. The sign conventions for the electromagnetic and strong couplings correspond to the covariant derivative $D_\mu = \partial_\mu + ieQ_f A_\mu + igT^a A^a_\mu$. With these definitions the coefficients $C_{7,8}$ are negative in the Standard Model, which is the choice generally adopted in the literature. The effective hamiltonian for $b \to d\gamma\gamma$ is obtained from (2.1)–(2.10) by the replacement $s \to d$. The Wilson coefficients C_i in (2.1) are known at next-to-leading order [7].

The amplitude for the $B \to \gamma\gamma$ decay has the general structure

$$\begin{aligned} \mathcal{A}\left(\bar{B} \to \gamma(k_1,\epsilon_1)\gamma(k_2,\epsilon_2)\right) &\equiv \frac{G_F}{\sqrt{2}} \frac{\alpha}{3\pi} f_B \frac{1}{2} \langle \gamma\gamma | A_+ F_{\mu\nu} F^{\mu\nu} - i \, A_- F_{\mu\nu} \tilde{F}^{\mu\nu} | 0 \rangle \\ &= \frac{G_F}{\sqrt{2}} \frac{\alpha}{3\pi} f_B \Big[A_+ \left(2k_1 \cdot \epsilon_2 \, k_2 \cdot \epsilon_1 - m_B^2 \epsilon_1 \cdot \epsilon_2 \right) - \\ &\qquad - 2i \, A_- \varepsilon(k_1, k_2, \epsilon_1, \epsilon_2) \Big] \, . \end{aligned} \tag{2.11}$$

Here $F^{\mu\nu}$ and $\tilde{F}^{\mu\nu}$ are the photon field strength tensor and its dual, where

$$\tilde{F}^{\mu\nu} = \frac{1}{2} \varepsilon^{\mu\nu\lambda\rho} F_{\lambda\rho} \tag{2.12}$$

with $\varepsilon^{0123} = -1$. The decay rate is then given by

$$\Gamma(\bar{B} \to \gamma\gamma) = \frac{G_F^2 m_B^3 f_B^2 \alpha^2}{288\pi^3} \left(|A_+|^2 + |A_-|^2 \right) . \tag{2.13}$$

In the heavy-quark limit we propose a factorization formula for the hadronic matrix elements of the operators in (2.1):

$$\langle \gamma(\epsilon_1)\gamma(\epsilon_2) | Q_i | \bar{B} \rangle = f_B \int_0^1 d\xi \, T_i^{\mu\nu}(\xi) \, \Phi_B(\xi) \epsilon_{1\mu} \epsilon_{2\nu} \tag{2.14}$$

where the ϵ_i are the polarization 4-vectors of the photons and $\Phi_B \equiv \Phi_{B1}$ is the leading twist light-cone distribution amplitude of the B meson. The latter quantity is a universal, nonperturbative object. It is defined via the light-cone projector for the B meson at leading power [24]

$$\langle 0 | b(0) \bar{q}(z) | \bar{B}(p) \rangle = \frac{i f_B}{4} (\not{p} + m_b) \gamma_5 \int_0^1 d\xi \, e^{-i\xi p_+ z_-} [\Phi_{B1}(\xi) + \not{n} \Phi_{B2}(\xi)] \, . \tag{2.15}$$

JHEP08(2002)054

The functions $\Phi_{B1,B2}(\xi)$ describe the distribution of light-cone momentum fraction $\xi = l_+/p_+$ of the spectator quark q with momentum l inside the B meson (only Φ_{B1} contributes in 2.14). Here light-cone components of four-vectors v are defined by

$$v_\pm = \frac{v^0 \pm v^3}{\sqrt{2}}\,. \tag{2.16}$$

The wave functions are highly asymmetric with $\xi = \mathcal{O}(\Lambda_{QCD}/m_b)$. They are normalized as

$$\int_0^1 d\xi\, \Phi_{B1}(\xi) = 1 \qquad \int_0^1 d\xi\, \Phi_{B2}(\xi) = 0\,. \tag{2.17}$$

If the light-like vector n in (2.15) is chosen appropriately parallel to one of the 4-momenta of the photons, only the first negative moment of $\Phi_{B1}(\xi)$ appears, which we parametrize by a quantity $\lambda_B = \mathcal{O}(\Lambda_{QCD})$, i.e.

$$\int_0^1 d\xi \frac{\Phi_{B1}(\xi)}{\xi} = \frac{m_B}{\lambda_B}\,. \tag{2.18}$$

Because there are no hadrons in the final state, only one type of hard-scattering kernel T (type II or hard-spectator contribution [8, 24]) enters the factorization formula. The QCD factorization formula (2.14) holds up to corrections of relative order Λ_{QCD}/m_b. The form of (2.14) with a simple convolution over the light-cone variable ξ is appropriate for the lowest (leading logarithmic) order in α_s, which we will use in the present analysis. A generalization to include transverse-momentum variables is likely to be necessary at higher orders in QCD [24, 26, 27, 28].

We conclude this section with a brief discussion of CP violation in $B \to \gamma\gamma$. The subscripts $\pm$ on $A_\pm$, defined in (2.11) for $\bar{B} \to \gamma\gamma$, denote the CP properties of the corresponding two-photon final states, which are eigenstates of CP: $A_{CP=+1}$ is proportional to the parallel spin polarization $\vec{\epsilon}_1 \cdot \vec{\epsilon}_2$ and $A_{CP=-1}$ is proportional to the perpendicular spin polarization $\vec{\epsilon}_1 \times \vec{\epsilon}_2$ of the photons. In addition to $A_\pm$ we introduce the CP conjugated amplitudes $\bar{A}_\pm$ for the decay $B \to \gamma\gamma$ (decaying $\bar{b}$ anti-quark). Then the deviation of the ratios

$$r^\pm_{CP} = \frac{|A_\pm|^2 - |\bar{A}_\pm|^2}{|A_\pm|^2 + |\bar{A}_\pm|^2} \tag{2.19}$$

from zero is a measure of direct CP violation. We shall focus here on this direct effect, which is specific for the $B \to \gamma\gamma$ decay, and will not consider CP violation originating in B–$\bar{B}$ mixing.

Due to the unitarity of the CKM matrix we can parametrize

$$A_\pm = \lambda_u a_u^\pm e^{i\alpha_u^\pm} + \lambda_c a_c^\pm e^{i\alpha_c^\pm} \tag{2.20}$$

$$\bar{A}_\pm = \lambda_u^* a_u^\pm e^{i\alpha_u^\pm} + \lambda_c^* a_c^\pm e^{i\alpha_c^\pm} \tag{2.21}$$

where $a^\pm_{u,c}$ are real hadronic matrix elements of weak transition operators and the $\alpha^\pm_{u,c}$ are their CP-conserving phases. We then have

$$r^\pm_{CP} = \frac{2\,\mathrm{Im}(\lambda_u\lambda_c^*) a_u^\pm a_c^\pm \sin(\alpha_c^\pm - \alpha_u^\pm)}{|\lambda_u|^2 a_u^{\pm 2} + |\lambda_c|^2 a_c^{\pm 2} + 2\,\mathrm{Re}(\lambda_u\lambda_c^*) a_u^\pm a_c^\pm \cos(\alpha_c^\pm - \alpha_u^\pm)}\,. \tag{2.22}$$

JHEP08(2002)054

The weak phase differences read

$$\mathrm{Im}(\lambda_u^{(q)}\lambda_c^{(q)*}) = \mp|\lambda_u^{(q)}||\lambda_c^{(q)}|\sin\gamma \tag{2.23}$$

with the negative sign for $q = s$ and the positive sign for $q = d$. The strong phase differences $\sin(\alpha_c^{\pm} - \alpha_u^{\pm})$ arise from final state interaction (FSI) effects, generated for instance via the Bander-Silverman-Soni (BSS) mechanism [29].

3. $B \to \gamma\gamma$ at leading power

To leading power in Λ_{QCD}/m_b and in the leading logarithmic (LL) approximation of QCD only one diagram contributes to the amplitude for $B \to \gamma\gamma$. It is the one-particle reducible (1PR) diagram with the electromagnetic penguin operator Q_7, where the second photon is emitted from the s-quark line. An illustration is given in figure 1. Evaluating the factorization formula (2.14) for this diagram leads to the matrix element

$$\langle\gamma(k_1,\epsilon_1)\gamma(k_2,\epsilon_2)|Q_7|\bar{B}\rangle = i\frac{f_B\alpha}{\pi}Q_s\int_0^1 d\xi\,\frac{\Phi_{B1}(\xi)}{\xi}\Big(2k_1\cdot\epsilon_2 k_2\cdot\epsilon_1 - m_B^2\epsilon_1\cdot\epsilon_2 - \\ - 2i\,\varepsilon(k_1,k_2,\epsilon_1,\epsilon_2)\Big) \tag{3.1}$$

Together with (2.1) and the definition of $A_{\pm}$ in (2.11) this implies

$$A_{\pm} = \lambda_t^{(q)} C_7 \frac{m_B}{\lambda_B} \tag{3.2}$$

where CKM unitarity, $\lambda_u^{(q)} + \lambda_c^{(q)} = -\lambda_t^{(q)}$, has been used. After summing over the photon polarizations the branching fraction to leading power becomes

$$B(B_q \to \gamma\gamma) = \tau_{B_q}\frac{G_F^2 m_{B_q}^5}{192\pi^3}|\lambda_t^{(q)}|^2 C_7^2 \frac{4\alpha^2 f_{B_q}^2}{3\lambda_{B_q}^2} \tag{3.3}$$

where $q = d, s$ for the decay of a B_d or a B_s meson, respectively.

In the present approximation the strong-interaction matrix elements multiplying $\lambda_u^{(q)}$ and $\lambda_c^{(q)}$ are identical and have no relative phase. The CP-violating quantities $r_{CP}^{\pm}$ defined in (2.19) therefore vanish for the strictly leading-power result.

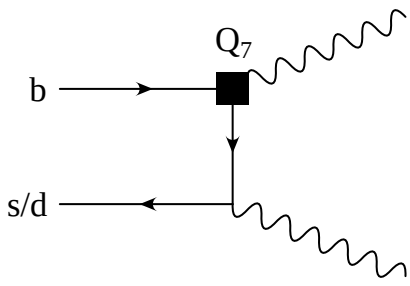

Figure 1: The leading power contribution to the $B \to \gamma\gamma$ amplitude given by the magnetic penguin operator Q_7. The diagram with interchanged photons is not shown. Radiation from the b-quark line (figure 2) is power suppressed.

JHEP08(2002)054

One may compare the behaviour of the $B \to \gamma\gamma$ decay amplitude in the heavy-quark limit with that of the rare decays $B \to V\gamma$ (with V a vector meson) and $B \to \pi\pi$. Disregarding CKM factors we can write

$$\begin{aligned}
\mathcal{A}(B \to \gamma\gamma) &\sim G_F\ e^2\ f_B A_\pm m_B^2 &&\sim G_F\ e^2\ \Lambda^{1/2} m_b^{5/2} \\
\mathcal{A}(B \to V\gamma) &\sim G_F\ e\ m_b F_V m_B^2 &&\sim G_F\ e\ \Lambda^{3/2} m_b^{3/2} \\
\mathcal{A}(B \to \pi\pi) &\sim G_F\ e^0\ f_\pi F^{B\to\pi} m_B^2 &&\sim G_F\ e^0\ \Lambda^{5/2} m_b^{1/2}
\end{aligned} \tag{3.4}$$

where we have used that the form factors scale as ($\Lambda = \Lambda_{QCD}$)

$$A_\pm \sim \frac{m_b}{\Lambda} \qquad f_B \sim \frac{\Lambda^{3/2}}{m_b^{1/2}} \qquad F_V \sim F^{B\to\pi} \sim \frac{\Lambda^{3/2}}{m_b^{3/2}}\,. \tag{3.5}$$

We observe that the ratio of the three amplitudes in (3.4) is $1 : (\Lambda/m_b) : (\Lambda/m_b)^2$. Thus $\mathcal{A}(B \to \gamma\gamma)$ is leading in the heavy-quark limit, while the other two are successively stronger suppressed. However, this hierarchy is compensated by the opposite pattern $e^2 : e : 1$ in the electromagnetic coupling e.

4. Contributions to $B \to \gamma\gamma$ with power suppression

Subleading contributions come from the 1PR diagram, where the second photon is emitted off the b quark line (figure 2), and from the one-particle irreducible diagram (1PI) (see figure 3).

To estimate the subleading 1PR contribution, we simply evaluate the graphs in figure 2 using the B-meson projector in (2.15). The result equals λ_B/m_B times the leading-power expression in (3.1), clearly showing the power suppression of this mechanism. Other corrections of the same order can arise from higher-twist terms in the B-meson wave function. We shall neglect all those subleading terms for the matrix element of Q_7, keeping in mind that they could naturally contribute relative corrections of order $\sim 10\%$. We stress, however, that subleading effects in $\langle Q_7 \rangle$ contribute equally to the up- and charm-quark components of the amplitude (see (2.1)). Therefore they do not give rise, in particular, to relative FSI

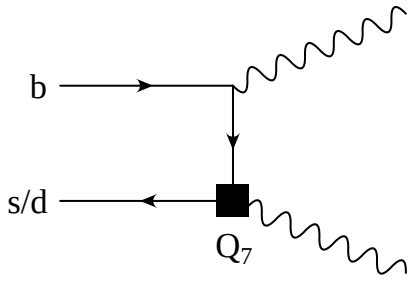

Figure 2: The subleading power 1PR diagram of the magnetic penguin operator Q_7. The diagram with interchanged photons is not shown.

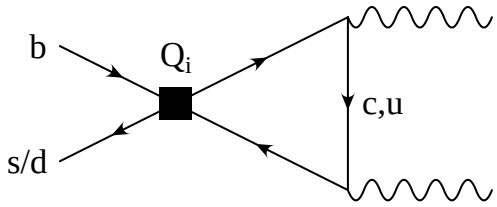

Figure 3: The subleading power 1PI diagram. Here the four-quark operators Q_i can contribute. The diagram with interchanged photons is not shown.

JHEP08(2002)054

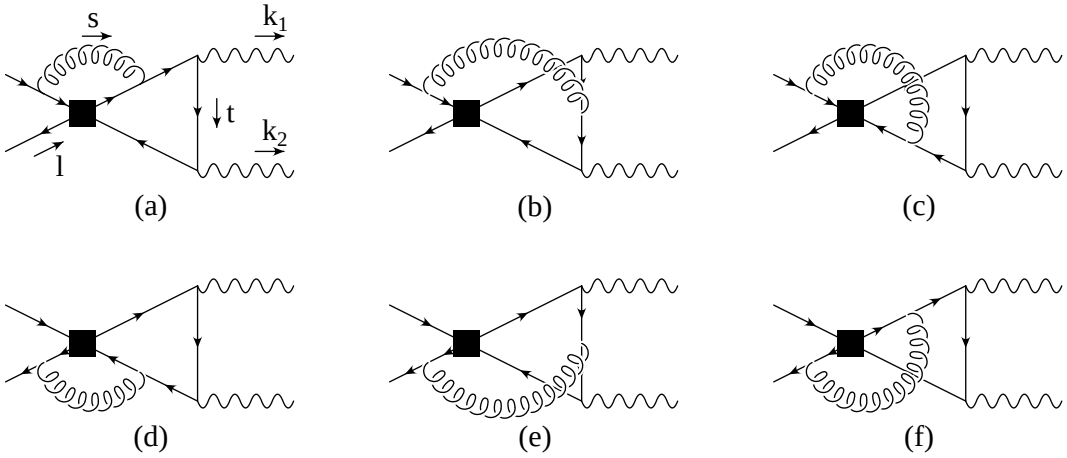

Figure 4: Gluon corrections to the 1PI diagram. Quark labels are as in figure 3 and the momentum assignment is everywhere as in diagram (a). The diagrams with interchanged photons are not shown.

phases between these sectors, which would affect direct CP violation. The same is true for perturbative QCD corrections to $\langle Q_7 \rangle$.

We next consider more closely the diagrams in figure 3. These 1PI contributions, which come from the matrix elements of four-quark operators in (2.1), are of special interest for two reasons. First, they are the basic effects responsible for a difference between the up- and charm-quark sectors of the amplitude, including rescattering phases. Second, they represent the parton-level processes that are dual to $B \to \gamma\gamma$ amplitudes from Q_i with hadronic intermediate states (J/Ψ, $D^{(*)}$, etc.), which are commonly considered as generic long-distance contributions. Investigating the amplitude in figure 3 will therefore shed light on this class of effects in $B \to \gamma\gamma$.

It shall now be argued that the 1PI contributions are calculable using QCD factorization. It is known that the one-loop contribution in figure 3 is free of infrared (IR) singularities. In addition we will show that also at $\mathcal{O}(\alpha_s)$ there are no collinear or soft IR divergences at leading power in $1/m_b$. By leading power we here mean the lowest non-vanishing order in the power expansion, where the entire 1PI contribution starts only at subleading power with respect to the dominant mechanism in figure 1. This suppression will be apparent from the explicit expressions given in (4.7) below. The relevant two-loop diagrams at $\mathcal{O}(\alpha_s)$ are shown in figure 4. Following the approach explained in the second reference of [24] for the case of $B \to D\pi$ decays, we demonstrate the absence of divergences for the hard-scattering part of the amplitude at $\mathcal{O}(\alpha_s)$. As a consequence the matrix elements of four-quark operators can be written in factorized form as in (2.14), where in the present case the kernel $T_i^{\mu\nu}$ is independent of ξ:

$$\langle \gamma(\epsilon_1)\gamma(\epsilon_2)|Q_{1,2}|\bar{B}\rangle = f_B T_{1,2}^{\mu\nu}\, \epsilon_{1\mu}\epsilon_{2\nu}\,. \tag{4.1}$$

The proof proceeds by identifying the potentially IR singular regions in the loop-momentum variables s and t and by determining the degree of IR divergence through power counting. We distinguish the following cases: (i) s, t soft, where all components

JHEP08(2002)054

scale like $s,\ t \sim \Lambda \ll m_b$. (ii) $s,\ t$ collinear with either photon momentum k_1 or k_2, for instance

$$s = \alpha k_1 + s_\perp + \alpha_2 k_2 \qquad\qquad t = \beta k_1 + t_\perp + \beta_2 k_2 \tag{4.2}$$

describing the region where s and t are collinear with k_1. Similar relations, with k_1 and k_2 interchanged, apply to the case where the loop momenta become collinear with k_2. The parameters in (4.2) scale as

$$\alpha, \beta \sim 1, \qquad s_\perp, t_\perp \sim \Lambda, \qquad \alpha_2, \beta_2 \sim \frac{\Lambda^2}{m_b^2} \tag{4.3}$$

and we have

$$k_{1,2}^2 = k_{1,2} \cdot s_\perp = k_{1,2} \cdot t_\perp = 0\,. \tag{4.4}$$

We consider explicitly the case where the quark inside the loop is massless, which is the most IR singular situation. The momentum l of the light external quark is counted as a soft quantity $l \sim \Lambda$. The dominant region for the diagrams in figures 3, 4 arises when both loop momenta are hard, $s,\ t \sim m_b$. The diagrams then scale as m_b. To demonstrate IR finiteness, one has to show that the potentially singular regions scale at least with one power of Λ and thus are suppressed relative to the hard contribution. Scaling as $\Lambda^0 m_b$ in a singular region would indicate a logarithmic divergence. The relevant cases for s and t are the soft-soft, soft-hard, hard-soft, collinear-collinear, collinear-hard, hard-collinear, soft-collinear and collinear-soft regions. For the collinear regions the momenta can be either $\sim k_1$ or $\sim k_2$. In the collinear-collinear case one needs to consider primarily that both momenta $\sim k_1$, or both $\sim k_2$. If one momentum is $\sim k_1$ and the other $\sim k_2$, the contribution is always less singular in the infrared. In the second reference of [24], besides the soft-collinear regions, a supersoft-collinear scaling had to be discussed, where $s,\ t \sim \Lambda^2$ for supersoft momenta. In the present context this scaling is not more singular than the soft-collinear one and will thus not be considered further.

Power counting then shows that all diagrams in figure 4 are IR finite at leading power in the soft-soft, soft-hard, hard-soft, collinear-hard, hard-collinear, soft-collinear and collinear-soft regions. In some cases one encounters a superficial logarithmic divergence, which vanishes when the relations $k_{1,2}^2 = 0$ and $k_1 \cdot \epsilon_1 = k_2 \cdot \epsilon_2 = 0$ are used.

On the other hand, in the collinear-collinear region (superficial) linear divergences $\sim \Lambda^{-1}$ may appear. An example is diagram (f) in figure 4 when both s and t are collinear to k_1. The diagram has the form

$$D_{(f)} = d^4s\, d^4t \frac{\gamma_\sigma(\not{l} - \not{s})\gamma^\lambda(1-\gamma_5)(\not{t} - \not{k}_2)\gamma_\nu\, \not{n}\gamma_\mu(\not{t} + \not{k}_1)\gamma^\sigma(\not{t} + \not{k}_1 - \not{s})\gamma_\lambda(1-\gamma_5)}{s^2\,(l-s)^2\,(t-k_2)^2\,t^2\,(t+k_1)^2\,(t+k_1-s)^2}\,. \tag{4.5}$$

Expanding the numerator in powers of Λ using (4.2) one finds that the superficial linear divergence drops out. This leads to

$$D_{(f)} = d^4s\, d^4t \frac{\gamma_\sigma(\not{l} - \not{s})}{(l-s)^2}\Gamma_R\, k_1^\sigma \tag{4.6}$$

with the remainder of the diagram $\Gamma_R \sim \Lambda^{-7}$. Together with collinear phase space, $d^4s\, d^4t \sim \Lambda^8$, the integrand then appears to scale as $\Lambda^0 m_b$. In fact, since $\not{k}_1(\not{l} - \not{s}) \sim m_b\Lambda$,

JHEP08(2002)054

$(l-s)^2 \sim m_b\Lambda$ for $s = \alpha k_1 + \mathcal{O}(\Lambda)$, the contribution behaves only as $D_{(f)} \sim \Lambda$. In a similar way all other contributions from the collinear-collinear regions can be shown to be power-suppressed.

In addition to the graphs displayed in figure 4 there are also diagrams in which the gluon connects only to the lines inside the triangular quark loop (vertex and self-energy corrections). Also these diagrams are found to be IR finite at leading power.

Finally, in contrast, one-gluon exchange among the external lines does generate leading IR divergences. However, these singularities match those appearing in the perturbative evaluation of the B-meson decay constant f_B at the same order, in accordance with the factorization formula (4.1). This completes our proof that at $\mathcal{O}(\alpha_s)$ for the 1PI contribution there are no collinear or soft infrared divergences at leading power in $1/m_b$ in the hard-scattering kernel. It supports our claim that these diagrams are calculable using QCD factorization.

Evaluating the 1PI diagram in figure 3 we find the matrix elements

$$\left.\begin{matrix}\langle Q_1^p\rangle \\ \langle Q_2^p\rangle\end{matrix}\right\} = -\frac{f_{B_q}\alpha}{\pi} Q_u^2 g(z_p)\varepsilon(k_1,k_2,\epsilon_1,\epsilon_2)\left\{\begin{matrix}1\\ N\end{matrix}\right. \tag{4.7}$$

with

$$g(z) = -2 + 4z\left[L_2\left(\frac{2}{1-\sqrt{1-4z+i\epsilon}}\right) + L_2\left(\frac{2}{1+\sqrt{1-4z+i\epsilon}}\right)\right]. \tag{4.8}$$

Here

$$L_2(x) = -\int_0^x dt \frac{\ln(1-t)}{t} \tag{4.9}$$

and $(p = u, c)$

$$z_p = \frac{m_p^2}{m_b^2}. \tag{4.10}$$

We note that the function $g(z)$ is related to the kernel $h(u,s)$ defined in [8] in the context of $B \to V\gamma$ by $g(z) = h(1,z)$. Real and imaginary part of $g(z)$ are displayed in figure 5. The function $g(z)$ is regular for $z \to 0$, $g(0) = -2$. Its value at $z = 1$ is $g(1) = 2(\pi^2 - 9)/9$, and $g(z) \to 0$ as $z \to \infty$. The function $g(z)$ has an imaginary part for $0 < z < 1/4$, which is maximal close to $z \approx 0.1$, the approximate physical value for the case of an internal charm quark. The imaginary part is due to the rescattering process $B \to p\bar{p} \to \gamma\gamma$ with an on-shell light-quark pair $p\bar{p}$ in the intermediate state. Since the process $B \to p\bar{p}$ is forbidden by helicity and angular momentum conservation for a massless quark p, the function $g(z)$ is real at $z = 0$ (that is for $p = u$). The helicity suppression of the phase will be absent at higher order in α_s.

Including the effect of 1PI diagrams in the decay amplitudes, the quantities $A_\pm$ from (3.2) become

$$A_+^p = -C_7\frac{m_B}{\lambda_B} \tag{4.11}$$

$$A_-^p = -C_7\frac{m_B}{\lambda_B} - \frac{2}{3}(C_1 + NC_2)g(z_p) \tag{4.12}$$

JHEP08(2002)054

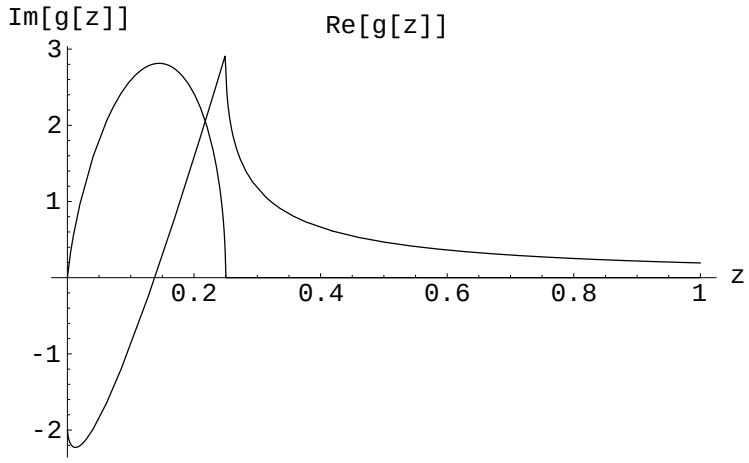

Figure 5: Real and imaginary part of $g(z)$.

where we have decomposed $A_\pm$ into

$$A_\pm = \sum_{p=u,c} \lambda_p^{(q)} A_\pm^p \,. \tag{4.13}$$

We see that only A_- is modified. The imaginary part of the 1PI loop diagram leads to a relative CP-conserving phase between the λ_u and the λ_c contribution. This gives a nonvanishing r_{CP}^- while r_{CP}^+ is still zero.

The effect of penguin operators $Q_3, \ldots, Q_6$ in the 1PI graphs is very small (at the percent level for the total amplitude) due to the small size of their Wilson coefficients. Also, they contribute equally to the up and charm sectors. We shall neglect them here. Their matrix elements can be found in [30].

5. Long-distance contributions to $B \to \gamma\gamma$ and $D \to \gamma\gamma$

We would next like to comment on the issue of long-distance effects and their relation with our analysis based on the heavy-quark limit. Long-distance contributions were calculated for both $B \to \gamma\gamma$ [15, 31, 32] and $D \to \gamma\gamma$ [33, 34]. The following mechanisms have been considered:

- B and $D \to V\gamma$, with a light vector meson V, followed by a $V \to \gamma$ conversion with the conversion factor supplied by the vector meson dominance (VMD) model. This gives a long-distance contribution to the matrix element of operator Q_7. Counting powers of m_b in the explicit result for the $B_s \to \phi\gamma \to \gamma\gamma$ amplitude in [15] shows that it is suppressed with Λ_{QCD}/m_b compared to the leading power result from figure 1. However, this is only one among the possible subleading power mechanisms for $\langle Q_7 \rangle$. Another comes, for example, from the diagram in figure 2.

  We can apply a similar power counting to the $D \to \gamma\gamma$ VMD amplitude of [34]. In the limit of a heavy charm quark it is likewise power suppressed with Λ_{QCD}/m_c compared to the short-distance amplitude. The limit $m_c \gg \Lambda_{QCD}$ is certainly questionable,

JHEP08(2002)054

but has nevertheless proven successful in some applications to charmed hadrons [35]. Again, the VMD contributions are just one out of several possible power corrections to the Q_7 matrix element.

- Single-particle unitarity contributions where the D^0 mixes with a spinless intermediate particle M, which then decays into a photon pair, $D^0 \to M \to \gamma\gamma$. As far as the quark-level topology is concerned, such a process corresponds to the 1PI contribution in figure 3. Relative to this contribution the amplitudes in [34] are at most of the same order in powers of the inverse heavy charm quark mass.

- Two-particle unitarity contributions are other hadron-level counterparts of the 1PI diagrams. Triangle loops with intermediate $D_s^{(*)}$ [31, 32] and $K^{(*)}$ [34] mesons were calculated for $B_s \to \gamma\gamma$ and $D \to \gamma\gamma$, respectively. As we will see in the next section, the effect of the 1PI contributions in $B \to \gamma\gamma$ on the decay amplitude is small. The authors of [32] also get a not too large effect in their reestimate of the result of [31], which had suggested a more sizable long-distance contribution. Yet, one has to keep in mind that the effects from intermediate D and D^* mesons are only two of many possible hadronic intermediate states. Since the meson model calculations are not based on a systematic approximation, it is for instance conceivable that cancellations required by quark-hadron duality would be missed. This could then lead to an overestimate of the effect.

  With obvious replacements we can use our 1PI results in (4.7) - (4.13) to estimate the quark-level analogue of the two-particle unitarity contributions to $D \to \gamma\gamma$ calculated in [34]. We obtain for the 1PI amplitude

$$\begin{aligned} A_{\rm 1PI}^{D\to\gamma\gamma} &= \frac{G_F}{\sqrt{2}}\frac{\alpha}{\pi} f_D Q_d^2 (C_1 + N C_2) |V_{cs}||V_{us}| \left[g\left(\frac{m_s^2}{m_c^2}\right) - g\left(\frac{m_d^2}{m_c^2}\right)\right] i\varepsilon(\epsilon_1,\epsilon_2,k_1,k_2) \\ &\approx -2.4\cdot 10^{-11}\,\text{GeV}^{-1}\,[-0.2+0.5i]\,\varepsilon(\epsilon_1,\epsilon_2,k_1,k_2) \\ \left|A_{\rm 1PI}^{D\to\gamma\gamma}\right| &\approx 1.3\cdot 10^{-11}\,\text{GeV}^{-1}\,|\varepsilon(\epsilon_1,\epsilon_2,k_1,k_2)| \end{aligned} \tag{5.1}$$

  where we set $f_D = 200\,\text{MeV}$, $m_s = 120\,\text{MeV}$, $m_d = 0$ and evaluated the Wilson coefficients at m_c. The contributions of a strange quark and a down quark in the loop are accompanied by CKM elements that are practically equal in absolute value, but opposite in sign. This leads to a strong GIM cancellation in the square bracket. Note that

$$g(z) = -2 + (-2\ln^2 z + 2\pi^2 - 4\pi\, i\, \ln z)z + \mathcal{O}(z^2)\,. \tag{5.2}$$

  The GIM mechanism removes the constant (-2) and gives an additional suppression $\sim 1/m_c^2$. Due to large logarithms $\ln z$ and numerical factors the suppression is relatively mild numerically. Also for the 1PR amplitude, the $c \to u\gamma$ transition exhibits a much stronger GIM cancellation than the corresponding process $b \to s\gamma$. In this case this has crucial consequences for the hierarchy of higher-order QCD terms. Leading logarithmic QCD corrections are known to enhance the $c \to u\gamma$ amplitude by more than an order of magnitude. Including the two-loop QCD contributions

JHEP08(2002)054

increases the amplitude by another two orders of magnitude [36]. Note however that the two-loop estimate from [36] shows a GIM cancellation pattern very similar to the 1PI amplitude in (5.1). In other words, the strong hierarchy of QCD corrections discussed in [36] is peculiar to the $c \to u\gamma$ transition. Hence, we do not expect a significant change from higher-order QCD corrections to (5.1). As a crude estimate, we therefore compare (5.1) with the $c \to u\gamma$ amplitude from the dominant two-loop diagrams of [36], which lead to an effective coefficient $|A| = 0.0047$ (entering the amplitude with a normalization corresponding to $|V_{cs}V_{us}C_7|$). We thus obtain for the "short-distance" amplitude (assuming $\lambda_D = 350\,\mathrm{MeV}$):

$$\begin{aligned} A_{\mathrm{SD}}^{D\to\gamma\gamma} &= -\frac{G_F}{\sqrt{2}}\frac{\alpha}{\pi} f_D\, 2Q_u\, A \frac{m_D}{\lambda_D}\left[i\varepsilon(\epsilon_1,\epsilon_2,k_1,k_2) - k_1\cdot\epsilon_2\, k_2\cdot\epsilon_1 + \frac{m_D^2}{2}\epsilon_1\cdot\epsilon_2\right] \\ \left|A_{\mathrm{SD},-}^{D\to\gamma\gamma}\right| &\approx 12.8\cdot 10^{-11}\mathrm{GeV}^{-1}|\varepsilon(\epsilon_1,\epsilon_2,k_1,k_2)|\,. \end{aligned} \tag{5.3}$$

We see that the 1PI amplitude, in this rough order-of-magnitude estimate, is smaller than the CP-odd part of the short-distance amplitude.

The authors of [34], on the other hand, find a large effect on the $D \to \gamma\gamma$ branching ratio from K^+K^- intermediate states. Their amplitude, however, is formally suppressed with $1/m_c$ relative to our 1PI amplitude. In view of our estimate above the large effect could be overrated. Only one intermediate state was taken into account so that important contributions in the duality sum might be missing.

- The decay mechanism $B_s \to \phi\psi \to \phi\gamma \to \gamma\gamma$ was estimated to give very small effects on the $B \to \gamma\gamma$ decay amplitudes [15]. It is power suppressed compared to the leading 1PR contribution.

6. Phenomenology

In this section we present numerical results for the expressions derived in this paper. Our choice of input parameters is summarized in table 1. For definiteness we employ the two-loop form of the running coupling $\alpha_s(\mu)$ (as quoted in [38]), which corresponds to $\alpha_s(M_Z) = 0.118$ for $\Lambda_{\overline{MS}}^{(5)} = 225\,\mathrm{MeV}$. With central values of all input parameters, at $\mu = m_b$, and using a nominal value of the CKM angle $\gamma = 58°$, we find for the branching ratios to leading logarithmic accuracy, evaluating (2.13), (4.11) – (4.13):

$$B(\bar{B}_s \to \gamma\gamma) = 1.23\cdot 10^{-6} \tag{6.1}$$

$$B(\bar{B}_d \to \gamma\gamma) = 3.11\cdot 10^{-8} \tag{6.2}$$

To display the size of power corrections from 1PI diagrams we compare A_+^p with A_-^p in (4.11) and (4.12) for $B_s \to \gamma\gamma$

$$A_+^u = 4.87 \qquad A_+^c = 4.87 \tag{6.3}$$

$$A_-^u = 5.29 \qquad A_-^c = 5.07 - 0.53\,i\,. \tag{6.4}$$

JHEP08(2002)054

CKM parameters and coupling constants					
V_{us}	V_{cb}	$\lvert V_{ub}/V_{cb}\rvert$	$\Lambda^{(5)}_{\overline{MS}}$	α	G_F
0.22	0.041	0.085 ± 0.025	225 MeV	1/137	$1.166 \times 10^{-5}\,\mathrm{GeV}^{-2}$

Parameters related to the B_d meson			
m_{B_d}	f_{B_d} [37]	τ_{B_d}	λ_{B_d}
5.28 GeV	(200 ± 30) MeV	1.55 ps	(350 ± 150) MeV

Parameters related to the B_s meson			
m_{B_s}	f_{B_s} [37]	τ_{B_s}	λ_{B_s}
5.37 GeV	(230 ± 30) MeV	1.49 ps	(350 ± 150) MeV

Quark and W-boson masses			
$m_b(m_b)$	$m_c(m_b)$	$m_t(m_t)$	M_W
4.2 GeV	(1.3 ± 0.2) GeV	166 GeV	80.4 GeV

Table 1: Summary of input parameters.

The calculable power corrections, which manifest themselves in the difference between A^p_+ and A^p_-, are of the expected canonical size of $\mathcal{O}(10\%)$. The precise value of these power-suppressed effects depends strongly on the renormalization scale μ. Typically, the relative size of the 1PI terms diminishes when the scale is lowered, both due to an increase in C_7, as well as due to the simultaneous decrease of the combination $C_1 + 3C_2$.

The main errors in (6.1)–(6.4) come from the variation of the nonperturbative input parameters λ_B and the decay constants f_{B_d} and f_{B_s} which are all poorly known and enter the branching ratios quadratically. The residual scale dependence is sizeable as well because we calculated at leading logarithmic accuracy only. The variation of the branching ratio with the scale would be less severe if next-to-leading QCD corrections were known. We expect the NLL corrections to increase the branching ratio as was the case for both the inclusive [7] and exclusive [8, 9] $b \to s\gamma$ decays.

The effect of next-to-leading logarithmic corrections for the branching ratio of $b \to s\gamma$ can be reproduced by choosing a low renormalization scale ($\mu \approx m_b/2$) in the leading logarithmic expressions. If such a low scale were also relevant for $B \to \gamma\gamma$ the branching ratios would read

$$\begin{aligned} B(\bar{B}_s \to \gamma\gamma)_{\mu=m_b/2} &= 1.53 \cdot 10^{-6} \\ B(\bar{B}_d \to \gamma\gamma)_{\mu=m_b/2} &= 4.08 \cdot 10^{-8} \end{aligned} \tag{6.5}$$

However, we prefer to use the nominal $\mu = m_b$ and to quote the standard scale ambiguity with $m_b/2 < \mu < 2m_b$ as a theoretical uncertainty.

For comparison we also show the results for the case where short-distance QCD effects are neglected altogether. This amounts to taking $\mu = M_W$ in the leading-order Wilson

JHEP08(2002)054

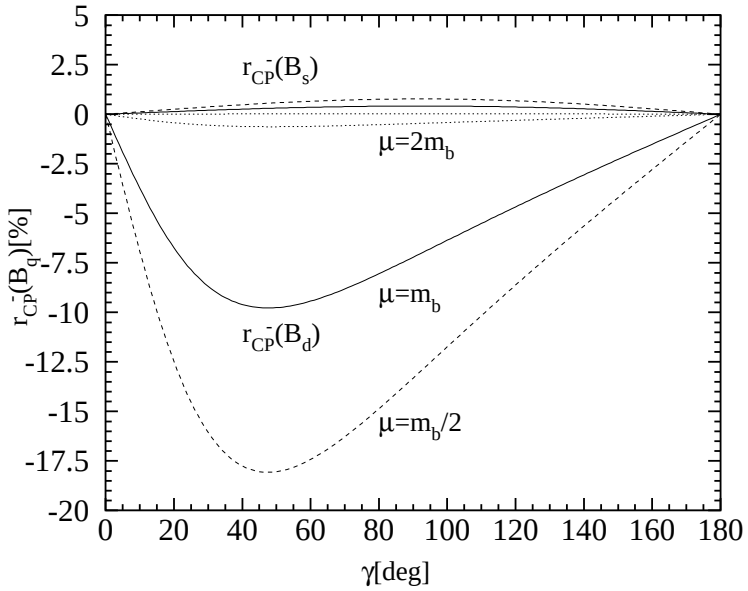

Figure 6: The CP-violating ratios r_{CP}^- for decays of neutral B_d and B_s mesons to two photons as a function of the CKM angle γ, each for three values of the renormalization scale $\mu = m_b/2$, m_b and $2m_b$.

coefficients and gives

$$\begin{aligned} B(\bar{B}_s \to \gamma\gamma)_{\mu=M_W} &= 0.60 \cdot 10^{-6} \\ B(\bar{B}_d \to \gamma\gamma)_{\mu=M_W} &= 1.22 \cdot 10^{-8} \end{aligned} \tag{6.6}$$

Clearly, the leading logarithmic QCD corrections yield a substantial enhancement [15, 17] of the branching ratios (6.1), (6.2), similar to the case of $b \to s\gamma$.

The numerical evaluation of (2.22) gives for central values of the input parameters and at $\mu = m_b$ the following predictions for the CP-violating ratios r_{CP}^-:

$$r_{CP}^-(B_s) = 0.35\% \tag{6.7}$$

$$r_{CP}^-(B_d) = -9.53\% \tag{6.8}$$

The effect is negligible for $B_s \to \gamma\gamma$ as expected. For $B_d \to \gamma\gamma$ CP violation occurs at the level of about 10%. It is interesting to note that in $B \to \gamma\gamma$ a non-vanishing CP asymmetry appears already at $\mathcal{O}(\alpha_s^0)$. This is possible via a modified BSS mechanism: Instead of the usual QCD penguin, already the electroweak loop in figure 3 itself leads to a CP-conserving phase.

The scale dependence of the CP asymmetry is rather strong, as can be seen in figure 6. The ratio r_{CP} also depends sensitively on fundamental CKM parameters such as the CKM angle γ (figure 6). The extremal value of $r_{CP}^-(B_d)$ is obtained for $\gamma = 50\,\text{deg}$. The sensitivity of the branching ratios and CP asymmetries to variations in the relevant input parameters is summarized in table 2. As already mentioned, the dominant uncertainty for our prediction of branching ratios comes from the variation of the hadronic

JHEP08(2002)054

	$B(\bar{B}_d \to \gamma\gamma)$ $[10^{-8}]$	$B(\bar{B}_s \to \gamma\gamma)$ $[10^{-6}]$	$r_{CP}^{-}(B_d)$ [%]	$r_{CP}^{-}(B_s)$ [%]
central	3.11	1.23	-9.53	0.35
λ_B	$+6.41/-1.58$	$+2.45/-0.61$	$+4.04/-3.91$	$+0.14/-0.15$
f_B	$+1.00/-0.86$	$+0.34/-0.30$	–	–
$\mu \in [m_b/2, 2m_b]$	$+0.97/-0.66$	$+0.31/-0.21$	$+8.91/-8.07$	$+0.30/-0.32$
m_c	$+0.10/-0.12$	$+0.03/-0.04$	$+1.75/-1.51$	$+0.05/-0.06$
$\gamma = (58 \pm 24)^\circ$	$+1.29/-0.96$	$+0.01/-0.02$	$+1.64/-0.25$	$+0.06/-0.12$

Table 2: Predictions for branching ratios and CP asymmetries with the errors from the individual input uncertainties.

parameter λ_B, which enters the leading-power amplitude. So far, our value for λ_B quoted in table 1 is only an educated guess with the uncertainty taken appropriately large. It would be highly desirable to get a better estimate of this important parameter. We anticipate that this problem can be addressed soon using QCD sum rules or lattice QCD. As λ_B parametrizes the first negative moment of the B meson wave function, it is a universal quantity that appears in many exclusive decays. An experimental determination might also be possible using radiative semileptonic B decays, or even a future measurement of $B \to \gamma\gamma$. The variation of the remaining parameters, other than λ_B, changes the branching ratios of $\bar{B}_d \to \gamma\gamma$ and $\bar{B}_s \to \gamma\gamma$ by about $\pm 50\%$ and $\pm 35\%$, respectively. If both branching fractions could be measured, one could consider their ratio where the dominant uncertainties from λ_B and f_B would cancel to a large extent. The main uncertainty for the CP asymmetries at present comes from the variation of the renormalization scale μ. This could be reduced, in principle, by including higher order QCD corrections.

Our predictions for the branching ratios are roughly two orders of magnitude below the current experimental bounds in (1.1). The recent upper limit for $B(B_d \to \gamma\gamma)$ from BaBar in (1.1) improved the previous limit from the L3 collaboration [11] by a factor of 20. With more integrated luminosity accumulated the upper bound will be further reduced, but it will barely reach the interesting region. The high-luminosity option SuperBaBar suggests a total integrated luminosity of 10 ab^{-1}. The number of observed $B_d \to \gamma\gamma$ events is then expected to be about two dozens for a branching fraction of $3 \cdot 10^{-8}$ [39]. Running such a machine at the $\Upsilon(5S)$ resonance would open the possibility of measuring $B_s \to \gamma\gamma$ as well. An interesting option might further be the operation of a future e^+e^- linear collider at the Z resonance.

7. Conclusions

In this paper we have presented a systematic discussion of the decays $B_{s,d} \to \gamma\gamma$, exploiting the simplifications of QCD in the heavy-quark limit. This enabled us to study these processes for the first time within a model-independent framework. In particular, we

JHEP08(2002)054

discussed the hierarchy of contributions to the decay amplitude in powers of Λ_{QCD}/m_b. The leading contribution to $B_s \to \gamma\gamma$ comes from the chromomagnetic $b \to s\gamma$ transition where the second photon is emitted from the s-quark constituent.

We have also investigated the $B \to \gamma\gamma$ matrix elements of four-quark operators Q_1 and Q_2, which proceed through 1PI triangular up- and charm-quark loops. These are suppressed by Λ_{QCD}/m_b relative to the leading contribution. Disregarding other terms of the same order, the consideration of these 1PI diagrams is nevertheless meaningful because they are the leading effects that induce a difference between the up- and charm-quark sectors of the amplitude. This is important for CP violation. They are also interesting as the partonic counterparts of certain, so-called long-distance effects in $B \to \gamma\gamma$ or, similarly, $D \to \gamma\gamma$. We have argued that the 1PI matrix elements are calculable in QCD factorization and have explicitly shown this property at leading ($\mathcal{O}(\alpha_s^0)$) and next-to-leading order ($\mathcal{O}(\alpha_s)$) in the strong coupling. Numerically the 1PI effect is only of order 10% in the amplitude, in accordance with a power-correction of canonical size.

Our estimates for branching ratios and CP asymmetries are given in table 2. At present there are still very large uncertainties in the absolute predictions for the branching fractions due to the high sensitivity on the hadronic parameter λ_B, which is a universal, process-independent property of the B meson. The quantity λ_B is poorly studied at present, but an improved determination should be possible in the future. Also, a measurement of $B_s \to \gamma\gamma$ could be a useful test of the hadronic dynamics and for λ_B, which plays an important role for many other exclusive B decays.

The experimental study of $B_{s,d} \to \gamma\gamma$ will not be easy. Presumably second generation B-factories or the high-intensity operation of a future e^+e^- linear collider at the Z pole would offer the best prospects. The radiative modes $B_{s,d} \to \gamma\gamma$ are interesting probes of heavy-flavour physics in their own right and especially in the context of factorization and the theory of exclusive B decays. In view of this, new ways towards their experimental observation should continue to be pursued.

References

[1] CLEO collaboration, S. Chen et al., *Branching fraction and photon energy spectrum for $b \to s\gamma$*, *Phys. Rev. Lett.* **87** (2001) 251807 [hep-ex/0108032].

[2] ALEPH collaboration, R. Barate et al., *A measurement of the inclusive $b \to s\gamma$ branching ratio*, *Phys. Lett.* **B 429** (1998) 169.

[3] Belle collaboration, K. Abe et al., *A measurement of the branching fraction for the inclusive $b \to X/s\gamma$ decays with belle*, *Phys. Lett.* **B 511** (2001) 151 [hep-ex/0103042].

[4] BaBar collaboration, B. Aubert et al., *$b \to s\gamma$ using a sum of exclusive modes*, hep-ex/0207074;
Determination of the branching fraction for inclusive decays $b \to X_s\gamma$, hep-ex/0207076.

[5] K. Adel and Y.-P. Yao, *Exact α_s calculation of $b \to s + \gamma$, $b \to s + g$*, *Phys. Rev.* **D 49** (1994) 4945 [hep-ph/9308349];
C. Greub and T. Hurth, *Two-loop matching of the dipole operators for $b \to s\gamma$ and $b \to s\ g$*, *Phys. Rev.* **D 56** (1997) 2934 [hep-ph/9703349];

JHEP08(2002)054

A.J. Buras, A. Kwiatkowski and N. Pott, *Next-to-leading order matching for the magnetic photon penguin operator in the $b \to X_s\gamma$ decay*, *Nucl. Phys.* **B 517** (1998) 353 [hep-ph/9710336].

[6] C. Greub, T. Hurth and D. Wyler, *Virtual $o(\alpha_s)$ corrections to the inclusive decay $b \to s\gamma$*, *Phys. Rev.* **D 54** (1996) 3350 [hep-ph/9603404];
A.J. Buras, A. Czarnecki, M. Misiak and J. Urban, *Two-loop matrix element of the current-current operator in the decay $b \to X_s\gamma$*, *Nucl. Phys.* **B 611** (2001) 488 [hep-ph/0105160].

[7] K.G. Chetyrkin, M. Misiak and M. Munz, *Weak radiative b-meson decay beyond leading logarithms*, *Phys. Lett.* **B 400** (1997) 206 [hep-ph/9612313], erratum *ibid.* **B425** (1998) 414.

[8] S.W. Bosch and G. Buchalla, *The radiative decays $B \to V\gamma$ at next-to-leading order in QCD*, *Nucl. Phys.* **B 621** (2002) 459 [hep-ph/0106081];
S.W. Bosch, *$B \to V\gamma$ at NLO from QCD factorization*, presented at the *Workshop on exclusive B decays*, 20-22 July 2001, Regensburg and at the *9th International Symposium on Heavy Flavor Physics (HF9)*, 10-13 September 2001, Caltech, Pasadena. To be published in the proceedings of HF9, edited by Anders Ryd, hep-ph/0109248.

[9] M. Beneke, T. Feldmann and D. Seidel, *Systematic approach to exclusive $B \to V\ell^+\ell^-$, $V\gamma$ decays*, *Nucl. Phys.* **B 612** (2001) 25 [hep-ph/0106067].

[10] A. Ali and A.Y. Parkhomenko, *Branching ratios for $B \to \rho\gamma$ decays in next-to- leading order in α_s including hard spectator corrections*, *Eur. Phys. J.* **C 23** (2002) 89 [hep-ph/0105302].

[11] L3 collaboration, M. Acciarri et al., *Search for the decays $B_d^0 \to \gamma\gamma$ and $B_s^0 \to \gamma\gamma$*, *Phys. Lett.* **B 363** (1995) 137.

[12] BABAR collaboration, B. Aubert et al., *Search for the decay $B^0 \to \gamma\gamma$*, *Phys. Rev. Lett.* **87** (2001) 241803 [hep-ex/0107068].

[13] G.L. Lin, J. Liu and Y.P. Yao, *Top quark mass dependence of the decay $B_s \to \gamma\gamma$ in the standard electroweak model*, *Phys. Rev.* **D 42** (1990) 2314.

[14] S. Herrlich and J. Kalinowski, *Direct CP-violation in $K, B \to \gamma\gamma$ with heavy top quark*, *Nucl. Phys.* **B 381** (1992) 501.

[15] G. Hiller and E.O. Iltan, *Leading logarithmic QCD corrections to the $B_s \to \gamma\gamma$ decay rate including long-distance effects through $B_s \to \phi\gamma \to \gamma\gamma$*, *Phys. Lett.* **B 409** (1997) 425 [hep-ph/9704385]; *Estimate of the long-distance contribution through $B \to s\psi$ to the $B_s \to \gamma\gamma$ decay rate*, *Mod. Phys. Lett.* **A 12** (1997) 2837 [hep-ph/9708477].

[16] L. Reina, G. Ricciardi and A. Soni, *QCD corrections to $b \to s\gamma\gamma$ induced decays: $B \to X_s\gamma\gamma$ and $B_s \to \gamma\gamma$*, *Phys. Rev.* **D 56** (1997) 5805 [hep-ph/9706253].

[17] C.-H.V. Chang, G.-L. Lin and Y.-P. Yao, *QCD corrections to $b \to s\gamma\gamma$ and exclusive $B_s \to \gamma\gamma$ decay*, *Phys. Lett.* **B 415** (1997) 395 [hep-ph/9705345].

[18] J.-j. Cao, Z.-j. Xiao and G.-r. Lu, *The $B \to X_s\gamma\gamma$ decay in the standard model and the general two-Higgs-doublet model*, *Phys. Rev.* **D 64** (2001) 014012 [hep-ph/0103154].

[19] J.O. Eeg, K. Kumericki and I. Picek, *The double radiative annihilation of the heavy-light fermion bound states*, *Fizika* **B10** (2001) 285–306 [hep-ph/0203055].

[20] G.G. Devidze, G.R. Dzhibuti and A.G. Liparteliani, *On the double radiative decays of the B_s meson and μ atom: $B_s \to \gamma\gamma$, $\mu^+e^- \to \gamma\gamma$*, *Nucl. Phys.* **B 468** (1996) 241.

JHEP08(2002)054

[21] H. Simma and D. Wyler, *Hadronic rare B decays: the case $b \to sgg$*, *Nucl. Phys.* **B 344** (1990) 283.

[22] T.M. Aliev and G. Turan, *$B_s \to \gamma\gamma$ decay in the two Higgs doublet model*, *Phys. Rev.* **D 48** (1993) 1176.

[23] Y. Dincer and L.M. Sehgal, *Charge asymmetry and photon energy spectrum in the decay $B_s \to \ell^+\ell^-\gamma$*, *Phys. Lett.* **B 521** (2001) 7 [hep-ph/0108144].

[24] M. Beneke, G. Buchalla, M. Neubert and C.T. Sachrajda, *QCD factorization for $B \to \pi\pi$ decays: strong phases and CP-violation in the heavy quark limit*, *Phys. Rev. Lett.* **83** (1999) 1914 [hep-ph/9905312]; *QCD factorization for exclusive, non-leptonic B meson decays: general arguments and the case of heavy-light final states*, *Nucl. Phys.* **B 591** (2000) 313 [hep-ph/0006124]; *QCD factorization in $B \to \pi K, \pi\pi$ decays and extraction of Wolfenstein parameters*, *Nucl. Phys.* **B 606** (2001) 245 [hep-ph/0104110].

[25] B. Grinstein, R.P. Springer and M.B. Wise, *Strong interaction effects in weak radiative anti-b meson decay*, *Nucl. Phys.* **B 339** (1990) 269;
Effective hamiltonian for weak radiative B meson decay, *Phys. Lett.* **B 202** (1988) 138.

[26] G.P. Korchemsky, D. Pirjol and T.-M. Yan, *Radiative leptonic decays of B mesons in QCD*, *Phys. Rev.* **D 61** (2000) 114510 [hep-ph/9911427].

[27] M. Beneke and T. Feldmann, *Symmetry-breaking corrections to heavy-to-light B meson form factors at large recoil*, *Nucl. Phys.* **B 592** (2001) 3 [hep-ph/0008255].

[28] C.W. Bauer, S. Fleming, D. Pirjol and I.W. Stewart, *An effective field theory for collinear and soft gluons: heavy to light decays*, *Phys. Rev.* **D 63** (2001) 114020 [hep-ph/0011336].

[29] M. Bander, D. Silverman and A. Soni, *CP noninvariance in the decays of heavy charged quark systems*, *Phys. Rev. Lett.* **43** (1979) 242.

[30] S.W. Bosch, *Exclusive radiative decays of B mesons in QCD factorization*, Ph.D. Thesis, MPI-PHT-2002-35.

[31] D. Choudhury and J.R. Ellis, *Estimates of long-distance contributions to the $B_s \to \gamma\gamma$ decay*, *Phys. Lett.* **B 433** (1998) 102 [hep-ph/9804300].

[32] W. Liu, B. Zhang and H.-q. Zheng, *On the long distance contribution to the $B_s \to \gamma\gamma$ decay in the effective lagrangian approach*, *Phys. Lett.* **B 461** (1999) 295 [hep-ph/9905504].

[33] S. Fajfer, P. Singer and J. Zupan, *The rare decay $D^0 \to \gamma\gamma$*, *Phys. Rev.* **D 64** (2001) 074008 [hep-ph/0104236].

[34] G. Burdman, E. Golowich, J. Hewett and S. Pakvasa, *Rare charm decays in the standard model and beyond*, *Phys. Rev.* **D 66** (2002) 014009 [hep-ph/0112235].

[35] M. Neubert, *Heavy quark symmetry*, *Phys. Rept.* **245** (1994) 259 [hep-ph/9306320].

[36] C. Greub, T. Hurth, M. Misiak and D. Wyler, *The $c \to u\gamma$ contribution to weak radiative charm decay*, *Phys. Lett.* **B 382** (1996) 415 [hep-ph/9603417].

[37] S.M. Ryan, *Heavy quark physics from lattice QCD*, *Nucl. Phys.* **106** *(Proc. Suppl.)* (2002) 86 [hep-lat/0111010].

[38] G. Buchalla, A.J. Buras and M.E. Lautenbacher, *Weak decays beyond leading logarithms*, *Rev. Mod. Phys.* **68** (1996) 1125 [hep-ph/9512380].

[39] *Physics at a 10^{36} asymmetric B factory*, SLAC-PUB-8970.

JHEP08(2002)054